Case Studies

Improved Differential Evolution with Collaborative Architecture for Bimetallic Cluster Structure Optimization

Xiaomin Wu, † Miao He, ‡ and Yousi Lin∗,†

†School of Opto-electronic and Communication Engineering, Xiamen University of Technology, Xiamen, China

‡ School of Electrical Engineering and Automation, Xiamen University of Technology, Xiamen, China

Case Study 1: Pt-Pd Bimetallic Clusters

We investigated platinum-palladium (Pt_xPd_y) bimetallic clusters with sizes N=13 and N=23 using density functional theory calculations to understand their composition-dependent energetic and structural properties.

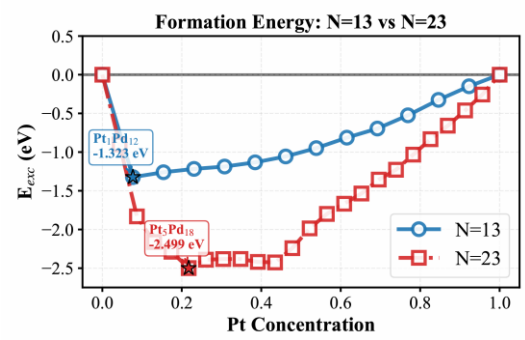

Figure 1a: Formation energy

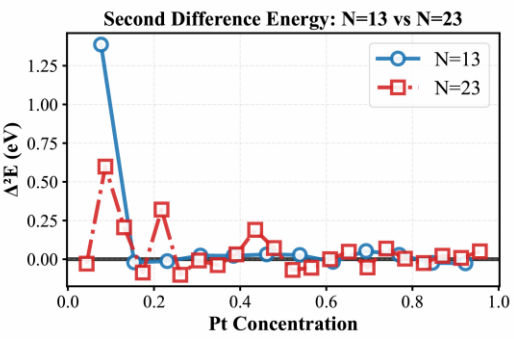

Figure 1b: Second difference energy

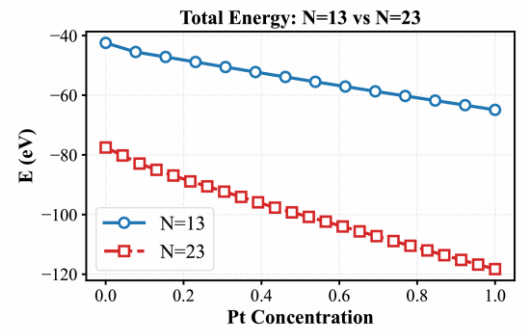

Figure 1c: Total energy comparison

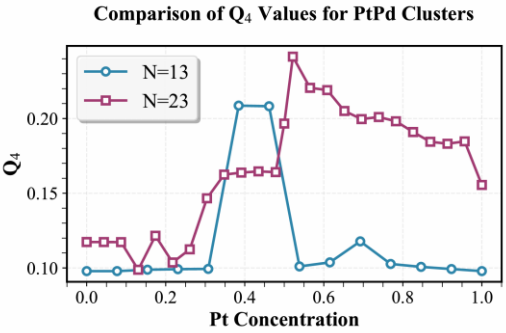

Figure 1d: Comparision of Q_4

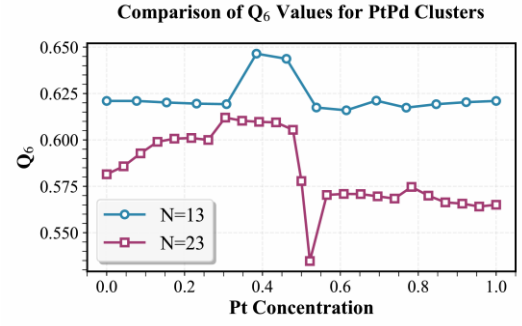

Figure 1e: Comparision of Q_6

Figure 1: Energetic and Structural Analysis of Pt_xPd_y Bimetallic Clusters (N=13 and N=23)

The formation energy profiles reveal that both cluster sizes exhibit clear energetic minima at Pd-rich compositions, with larger clusters showing deeper minima and thus enhanced thermodynamic stability through improved alloying effects. The negative formation energies across most compositions demonstrate that mixing is energetically favorable compared to phase-separated pure clusters. The second difference energy identifies distinct magic compositions where clusters show exceptional relative stability: smaller clusters display sharper, more pronounced stability peaks indicating well-defined magic compositions, while larger clusters exhibit multiple competitive peaks with a more continuous stability landscape, suggesting greater compositional flexibility. The asymmetric nature of the curves indicates that incorporating small amounts of Pt into Pd-rich clusters is particularly favorable, likely due to electronic effects and optimization of metal-metal bond strengths.

The total energy decreases systematically with increasing Pt concentration for both cluster sizes, reflecting the higher cohesive energy of platinum compared to palladium. The nearly monotonic but non-linear trends suggest good miscibility between the two metals throughout the composition range. Notably, larger clusters show a steeper energy gradient with composition, indicating that compositional changes have magnified energetic effects in larger systems, which has important implications for thermal stability and potential segregation behavior at elevated temperatures.

The structural order parameters reveal fundamentally different behaviors between cluster sizes: smaller clusters maintain nearly constant tetrahedral order parameter (Q_4) and consistently high icosahedral order parameter (Q_6) across all compositions, confirming robust icosahedral symmetry regardless of Pt/Pd ratio, while larger clusters show significantly higher and more variable Q_4 values with systematically lower Q_6 values, indicating greater structural complexity and composition-dependent distortions. This demonstrates that perfect icosahedral symmetry becomes increasingly difficult to maintain in larger clusters due to strain and packing constraints. The three-dimensional structural evolution reveals that both cluster sizes exhibit strong compositional segregation patterns rather than random mixing: Pt atoms consistently prefer high-coordination interior positions at low concentrations before gradually occupying surface sites, driven by platinum's higher cohesive energy and atomic size differences. Larger clusters show more pronounced segregation effects including distinct Janus-like structures at intermediate compositions where Pt and Pd form separate surface domains. These composition-dependent ordering patterns are crucial for catalytic applications as they directly control the distribution and nature of active surface sites.

The structural order parameters reveal fundamentally different behaviors between cluster sizes: smaller clusters maintain nearly constant tetrahedral order parameter (Q_4) and consistently high icosahedral order parameter (Q_6) across all compositions, confirming robust icosahedral symmetry regardless of Pt/Pd ratio, while larger clusters show significantly higher and more variable Q_4 values with systematically lower Q_6 values, indicating greater structural complexity and composition-dependent distortions. This demonstrates that perfect icosahedral symmetry becomes increasingly difficult to maintain in larger clusters due to strain and packing constraints. The three-dimensional structural evolution reveals that both cluster sizes exhibit strong compositional segregation patterns rather than random mixing: Pt atoms consistently prefer high-coordination interior positions at low concentrations before gradually occupying surface sites, driven by platinum's higher cohesive energy and atomic size differences. Larger clusters show more pronounced segregation effects including distinct Janus-like structures at intermediate compositions where Pt and Pd form separate surface domains. These composition-dependent ordering patterns are crucial for catalytic

applications as they directly control the distribution and nature of active surface sites.

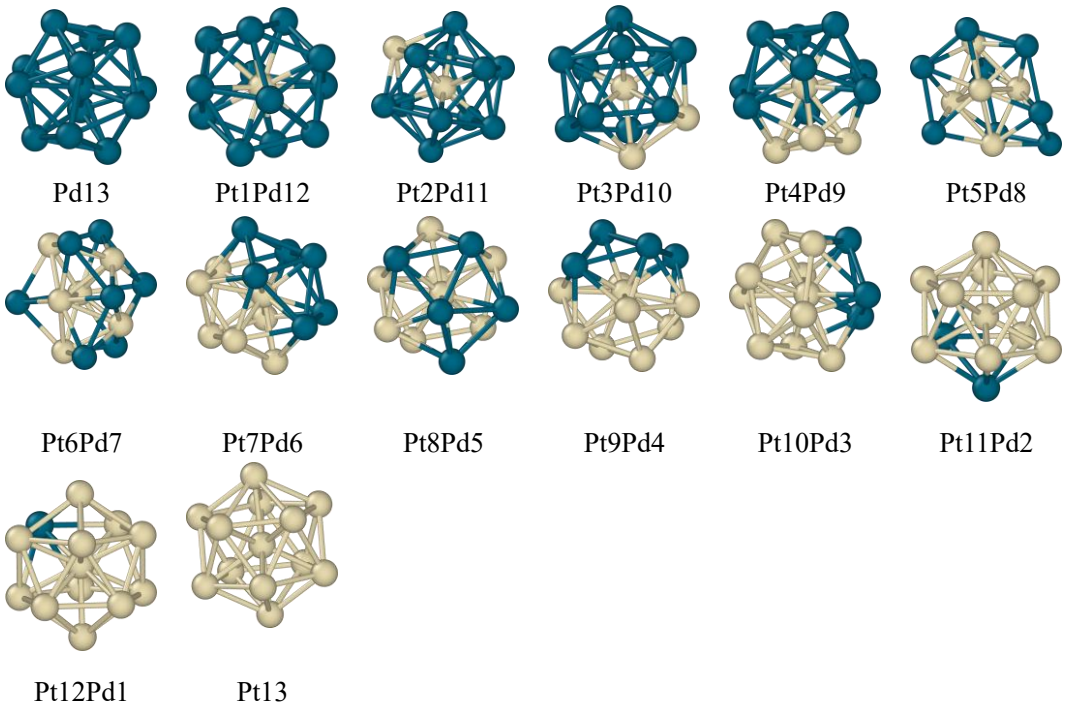

Figure 2: Structural Evolution of PtPd Bimetallic Clusters (N=13)

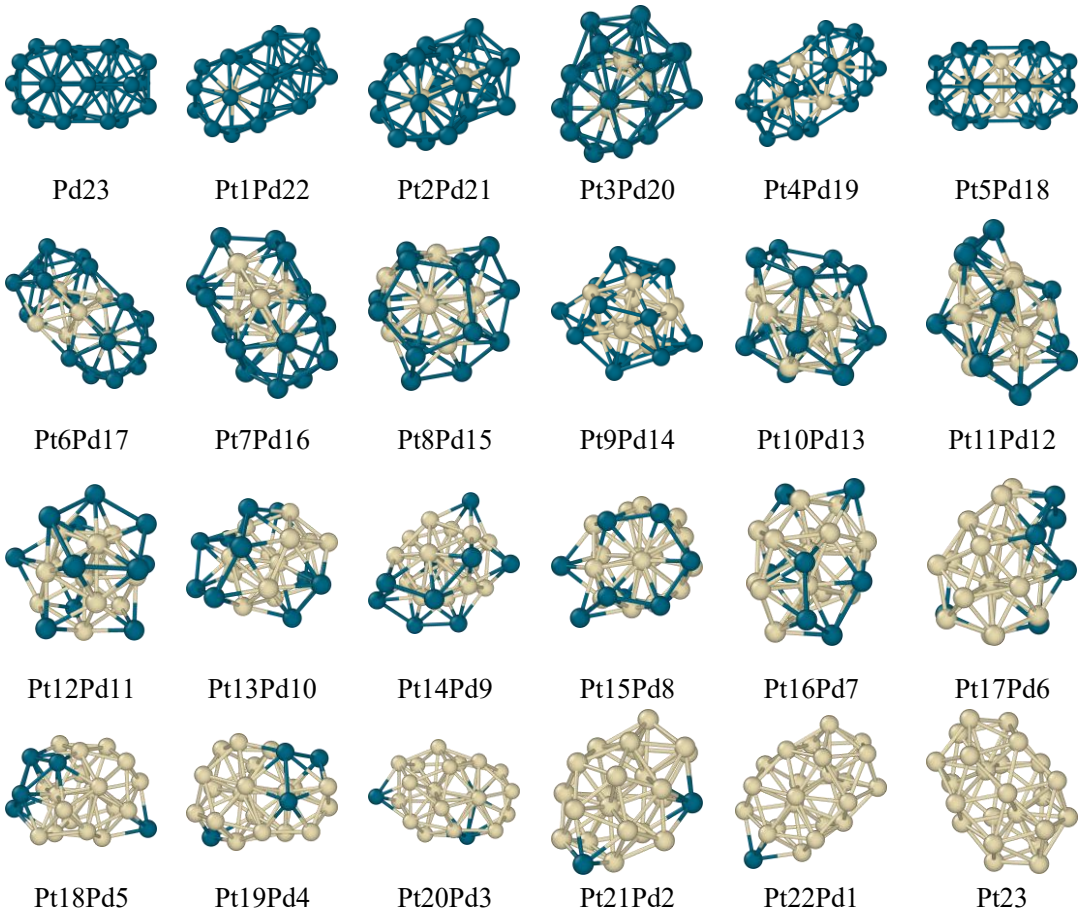

Figure 3: Structural Evolution of PtPd Bimetallic Clusters (N=23)

Our analysis reveals clear size-dependent stability patterns with distinct optimal compositions favoring Pd-rich clusters, where small clusters maintain rigid icosahedral structures while larger clusters display greater compositional flexibility and pronounced core-shell segregation. The identified magic compositions with enhanced relative stability provide promising targets for synthesizing monodisperse bimetallic nanoparticles. The observed Pd-rich compositions showing favorable mixing energies are particularly attractive for catalytic applications, offering an optimal balance between catalytic activity and cost-effectiveness, though future work should include temperature-dependent simulations and direct catalytic activity investigations for specific reactions.

Case Study 2: Cu-Ag Bimetallic Clusters

We investigated copper-silver (Cu_xAg_y) bimetallic clusters with sizes N=13 and N=23 using density functional theory calculations to understand their composition-dependent energetic and structural properties.

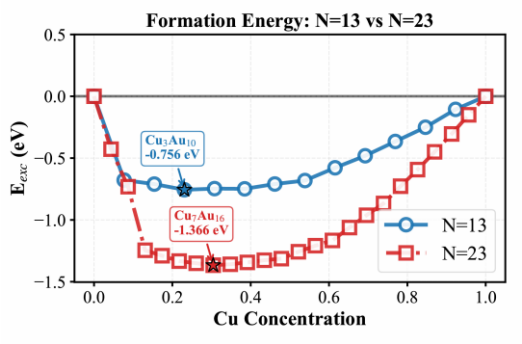

Figure 4a: Formation energy

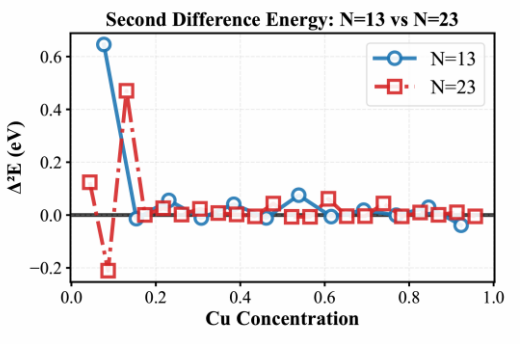

Figure 4b: Second difference energy

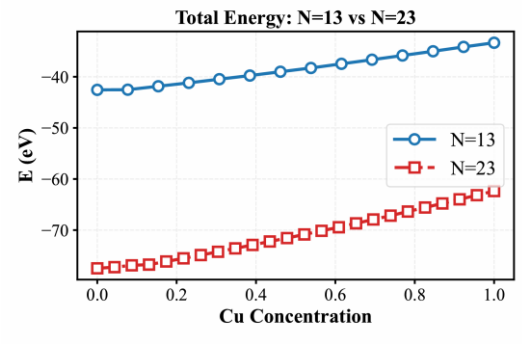

Figure 4c: Total energy comparison

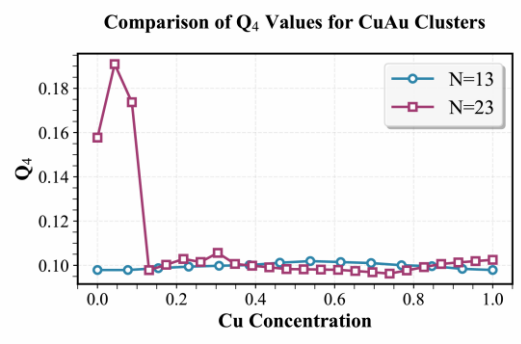

Figure 4d: Comparision of Q_4

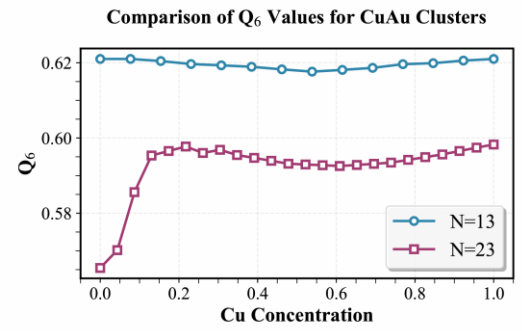

Figure 4e: Comparision of Q_6

Figure 4: Energetic and Structural Analysis ofCu_xAg_y Bimetallic Clusters (N=13 and N=23)

The formation energy profiles reveal that both cluster sizes exhibit clear energetic minima at Ag-rich compositions, with larger clusters showing deeper minima and thus enhanced thermodynamic stability through improved alloying effects. The negative formation energies across most compositions demonstrate that mixing is energetically favorable compared to phase-separated pure clusters, though the alloying tendency is weaker than in Pt-Pd systems. The second difference energy identifies distinct magic compositions where clusters show exceptional relative stability: smaller clusters display a sharp stability peak at very low Cu concentrations, indicating that single Cu atom doping provides optimal stability, while larger clusters exhibit broader peaks with greater compositional flexibility. The asymmetric nature of the curves indicates that incorporating small

amounts of Cu into Ag-rich clusters is particularly favorable, likely due to electronic effects and optimization of metal-metal bond strengths.

The total energy increases systematically with increasing Cu concentration for both cluster sizes, reflecting the lower cohesive energy of copper compared to silver. The nearly monotonic trends suggest good miscibility between the two metals throughout the composition range. Larger clusters show a steeper energy gradient with composition, indicating that compositional changes have magnified energetic effects in larger systems, which has important implications for thermal stability and potential segregation behavior at elevated temperatures.

The structural order parameters reveal fundamentally different behaviors between cluster sizes: smaller clusters maintain consistently low tetrahedral order parameter (Q_4) and high icosahedral order parameter (Q_6) across all compositions, confirming robust icosahedral symmetry regardless of Cu/Ag ratio, while larger clusters show a sharp Q_4 peak at very low Cu concentrations followed by rapid decrease, with slightly lower but well-maintained Q_6 values throughout. This demonstrates that N=13 clusters preserve rigid icosahedral geometry, while N=23 clusters exhibit composition-dependent local distortions yet maintain overall icosahedral character. The three-dimensional structural evolution reveals that Cu-Ag clusters exhibit compositional segregation patterns driven by atomic size differences: Cu atoms likely preferentially occupy interior positions at low concentrations due to their smaller atomic radius, forming core-shell structures that minimize strain. These composition-dependent ordering patterns are crucial for catalytic and plasmonic applications as they directly control the distribution and nature of active surface sites.

Our analysis reveals clear size-dependent stability patterns with distinct optimal compositions favoring Ag-rich clusters, where small clusters maintain rigid icosahedral structures while larger clusters display greater compositional flexibility and pronounced core-shell segregation. The identified magic compositions at Ag-rich regions provide promising targets for synthesizing monodisperse bimetallic nanoparticles. The observed Ag-rich compositions with dilute Cu doping are particularly attractive for plasmonic and catalytic applications, offering an optimal balance between performance and cost-effectiveness, though future work should include temperature-dependent simulations and direct activity investigations for specific applications.

Case Study 3: Pure Pt Clusters

We investigated pure platinum clusters with sizes N=13, 23, 38, 55, and 79 using density functional theory calculations to understand their size-dependent energetic and structural evolution.

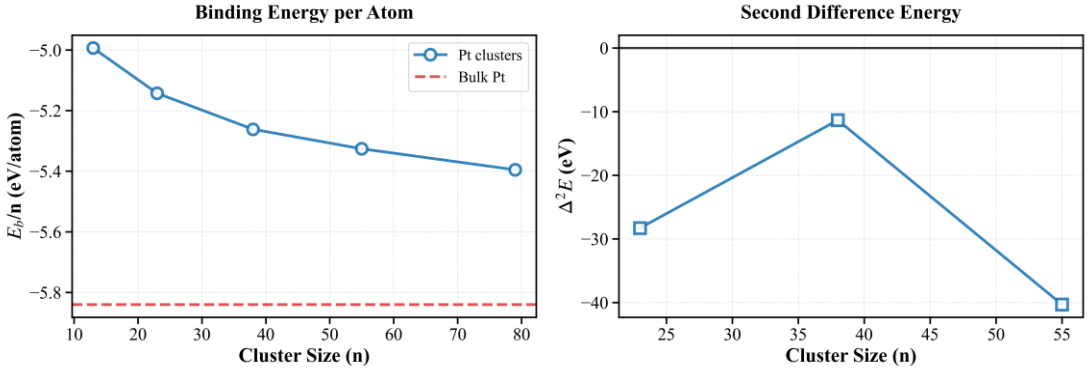

Figure 5: Size-dependent stability and thermodynamic properties of Pt clusters

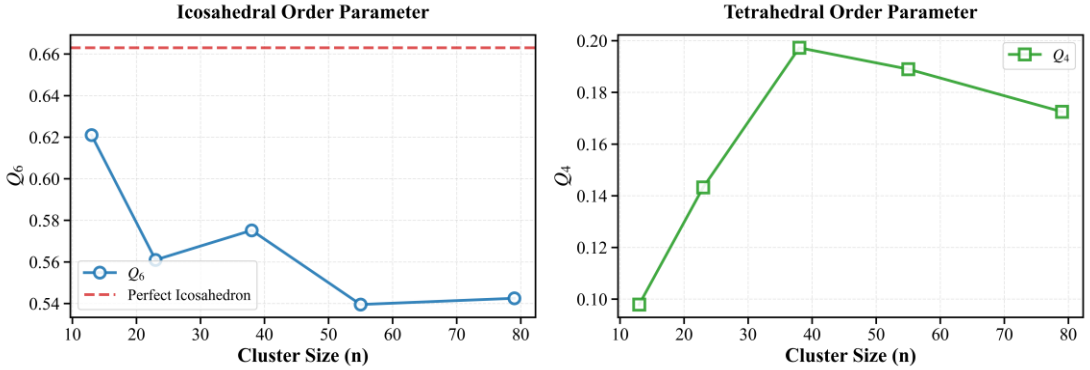

Figure 6: Evolution of structural order parameters with cluster size

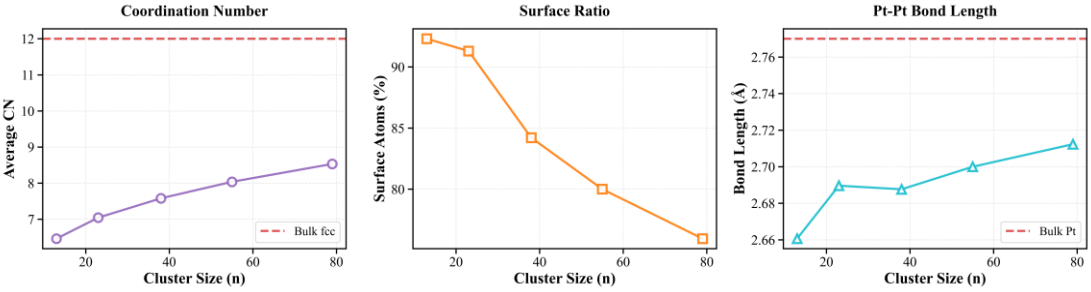

Figure 7: Geometric and structural characteristics of Pt clusters as a function of size

The binding energy per atom increases systematically with cluster size, evolving from -4.99 eV/atom for Pt_{13} to -5.40 eV/atom for Pt_{79}, demonstrating a clear convergence toward the bulk platinum cohesive energy of approximately -5.8 eV/atom. This trend reflects the decreasing influence of under-coordinated surface atoms as cluster size increases, with smaller clusters exhibiting relatively weaker binding due to their higher surface-to-volume ratios. The second difference energy analysis identifies Pt_{38} as a particularly stable magic number cluster, showing a pronounced stability peak that indicates exceptional thermodynamic favorability compared to neighboring sizes. This enhanced stability at N=38 suggests a geometrically optimal structure that minimizes strain and maximizes metal-metal bonding efficiency.

The structural order parameters reveal a fundamental transition in geometric character with

increasing cluster size. The icosahedral order parameter Q_6 remains high for small clusters, with Pt_{13} exhibiting nearly perfect icosahedral symmetry at Q_6=0.621, but systematically decreases and stabilizes around 0.54 for larger clusters, indicating a gradual departure from ideal icosahedral geometry toward more complex multi-shell arrangements. Conversely, the tetrahedral order parameter Q_4 shows an initial increase from 0.098 in Pt_{13} to a maximum of 0.197 in Pt_{38}, then slightly decreases and stabilizes around 0.17-0.19 for larger sizes, reflecting the emergence of local tetrahedral coordination environments in the transition regime between small icosahedral clusters and bulk-like structures. The coordination number increases systematically from 6.46 for Pt_{13} to 8.53 for Pt_{79}, approaching but not yet reaching the bulk fcc value of 12, while the surface ratio decreases predictably from 92.3% to 75.9%, confirming the growing importance of interior atoms with well-defined bulk-like coordination.

Our analysis demonstrates clear size-dependent evolution in both energetic stability and structural character, with the identification of Pt_{38} as a magic number providing valuable guidance for targeted synthesis of monodisperse platinum nanoparticles. The systematic convergence of binding energy, bond length, and coordination environment toward bulk values illustrates the nanoscale-to-bulk transition, while the persistent deviation from perfect bulk symmetry even at N=79 emphasizes the unique properties of nanoclusters. These findings are particularly relevant for catalytic applications where size-specific electronic and geometric effects directly influence activity and selectivity, though future work incorporating temperature effects and adsorbate interactions would provide more comprehensive insights into realistic catalytic conditions.

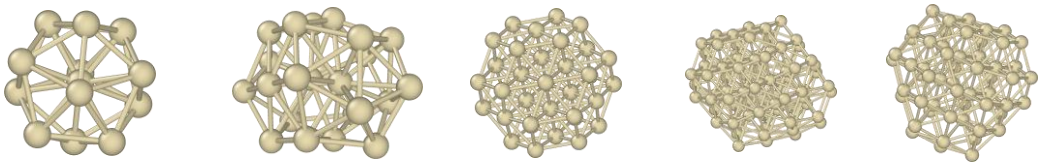

Pt13 Pt23 Pt38 Pt55 Pt79

Figure 8: Optimized structures of representative Pt clusters at different sizes